Geomechanics and Engineering, *Vol. 28, No. 3 (2022) 313-334*
https://doi.org/10.12989/gae.2022.28.3.313

Prediction of the static and dynamic mechanical properties of sedimentary rock using soft computing methods

Abiodun I. Lawal[1,2a], Sangki Kwon*[1], Adeyemi E. Aladejare[3b] and Gafar O. Oniyide[2c]

[1]*Department of Energy Resources Engineering, Inha University Yong-Hyun Dong, Nam Ku, Incheon, Korea*
[2]*Department of Mining Engineering, Federal University of Technology, Akure, Nigeria*
[3]*Oulu Mining School, University of Oulu, Finland*

(Received July 11, 2021, Revised December 8, 2021, Accepted December 13, 2021)

Abstract. Rock properties are important in the design of mines and civil engineering excavations to prevent the imminent failure of slopes and collapse of underground excavations. However, the time, cost, and expertise required to perform experiments to determine those properties are high. Therefore, empirical models have been developed for estimating the mechanical properties of rock that are difficult to determine experimentally from properties that are less difficult to measure. However, the inherent variability in rock properties makes the accurate performance of the empirical models unrealistic and therefore necessitate the use of soft computing models. In this study, Gaussian process regression (GPR), artificial neural network (ANN) and response surface method (RSM) have been proposed to predict the static and dynamic rock properties from the P-wave and rock density. The outcome of the study showed that GPR produced more accurate results than the ANN and RSM models. GPR gave the correlation coefficient of above 99% for all the three properties predicted and RMSE of less than 5. The detailed sensitivity analysis is also conducted using the RSM and the P-wave velocity is found to be the most influencing parameter in the rock mechanical properties predictions. The proposed models can give reasonable predictions of important mechanical properties of sedimentary rock.

Keywords: empirical models; Gaussian process regression; response surface method; rock properties

1. Introduction

Rocks are composed of different minerals component which makes it inhomogeneous and as a result, it exhibits wide range of variations in its properties. The rock properties can generally be physical or mechanical. These properties are required in both preliminary and detail designs of surface and underground mine including civil engineering excavations. For example, the stability of the rock slope, underground excavations, tunnels, dams, trenches, and caverns are based on rock properties (Khandelwal and Singh 2009). However, field engineers are usually faced with difficulties in assessing the properties of the rock. This is because the time, cost, accuracy, and expertise required to perform the experiments specifically for determination of mechanical properties are too high. As a result, there is large dependence on the estimation of rock mechanical properties to perform preliminary designs in civil and mining engineering applications.

Researchers have proposed numerous empirical models to predict the mechanical properties of rocks using physical properties (such as density, porosity, Schmidt rebound hardness etc.), mechanical properties (such as point load index, tensile strength, single compression strength index etc.) or combination of both (Aladejare *et al*. 2021). Some of the existing empirical equations for estimating the properties of sedimentary rocks are presented in Table 1. The equations are either one parameter or multi parameter-based equations. The most commonly measured or estimated mechanical properties of the rock is the uniaxial compressive strength (UCS) because it is largely required in civil and mining excavation design and also in rock mass classification systems such as rock mass rating (RMR) and Q-System meant to characterize the rocks for their suitability or stability (Aladejare 2020). The deformation properties of the rock such as Young's modulus is another important rock property that are required in performing various rock analysis, such as numerical modelling for the assessment of the stability of the excavations. The Young's modulus could either be static or dynamic but the empirical model for assessing the dynamic Young's modulus is scarce because of its dependent on the shear wave velocity which is difficult to measure (Aladejare *et al*. 2021).

Apart from the empirical models, soft computing techniques such as ANN, support vector regression (SVR), Fuzzy inference system (FIS), adaptive neuro fuzzy inference system (ANFIS), genetic programming (GP), particle swarm optimized ANN (PSO-ANN), imperialist competitive algorithm optimized ANN (ICA-ANN) and

*Corresponding author, Professor
E-mail: kwonsk@inha.ac.kr
[a]Ph.D.
E-mail: ailawal@futa.edu.ng
[b]Ph.D.
E-mail: adeyemi.aladejare@oulu.fi
[c]Ph.D.
E-mail: gooniyide@futa.edu.ng

ISSN: 2005-307X (Print), 2092-6219 (Online)

Table 1 Empirical models for estimating rock properties

S/N	Relationship	No of data	R^2	Rock types	Reference
1	UCS=0.1333V_p-227.19, MPa	12	0.96	Sed	Khandelwal and Singh (2009)
2	$UCS = 142.47 \times e^{(-9560.57/(\rho V_p))}$, MPa	64	0.75	Sed	Moradian and Behnia (2009)
3	UCS=17.6 $Is_{(50)}$ + 13.5, MPa	7	0.88	Sed	Aliyu *et al*. (2019)
4	UCS=-6.319+4.418×$10^{-3}V_p$+0.427γ, MPa	19	0.95	Sed	Dinçer *et al*. (2008)
5	UCS=-127.49+34.57ρ+0.022V_p, MPa	18	0.86	Sed	Jamshidi *et al*. (2018)
6	UCS=0.0465N^2-0.1756 N+27.682, MPa	41	0.86	Sed	Torabi *et al*. (2010)
7	UCS=3$V_p^4V_s^{-2.85}$, MPa	46	NA	Sed	Uyanik *et al*. (2019)
8	UCS=0.121SCSI-7.462D+63.98, MPa	10	0.66	Sed	Ashtari *et al*. (2019) (D = 3-10mm)
9	UCS=0.476PD-0.017CC-0.049Q+0.065, MPa	138	0.53	Sed (Sandstones)	Zorlu *et al*. (2008)
10	UCS=13.244$Is_{(50)}$+0.013V_p-16.987, MPa	40	0.95	Sed (Marlstone)	Azimian *et al*. (2014)
11	UCS=1.277N+2.186BPI+16.41$Is_{(50)}$+0.011V_p-82.436, MPa	108	0.91	Sed	Heidari *et al*. (2018)
12	UCS=0.035V_p+3.158I_{d2}-0.954ρ-342.729, MPa	94	0.94	Mix	Sharma *et al*. (2017)
13	UCS=-229+3.74N+76.2ρ-3.24n, MPa	93	0.90	Mix	Majdi and Rezaei (2013)
14	UCS=1.277N+2.86BPI+16.41$Is_{(50)}$+0.011V_p-82.436, MPa	53	0.91	Sed	Jalali *et al*. (2017)
15	UCS=34.186DD+0.838I_{d2}+2.308BTS-109.184, MPa	47	0.93	Sed	Armaghani *et al*. (2018)

UCS-uniaxial compressive strength, ρ-density, V_p-P-wave velocity, V_s- S-wave velocity, $Is_{(50)}$- Point load strength, N- Schmidt hardness number, SCSI- single compressive strength index, D-particle diameter, PD-Packing density, CC-concavo-convex, Q-quartz content, n-Porosity, Brazilian tensile strength (BTS), I_{d2}-slake durability index, γ-unit weights, Sed-sedimentary rock, Mix-mixed rock types

gene expression programming (GEP) have also been used to predict the mechanical properties of rocks or sandy soil (Yilmaz and Yuksek 2009, Majdi and Beiki 2010, Mohamad *et al*. 2015, Armaghani *et al*. 2015, 2016, 2018, 2021, Aboutaleb *et al*. 2018, Mohamad *et al*. 2018, Heidari *et al*. 2018, Ren *et al*. 2019, Luat *et al*. 2020, etc.). The performance of the soft computing (SC) model has been largely more accurate than the empirical model. Unlike the other aspects of mining engineering such as ground vibration prediction where Moth-flame optimized ANN (MFO-ANN), sine-cosine algorithm optimized ANN (SCA-ANN), Gaussian process regression (Lawal *et al*. 2021a, b) etc SC methods have been used, many SC methods are yet to be used in assessing the properties of rock and hence there is a need to try new techniques. This is because accurate assessment of the rock properties is required to avoid failure of rock engineering structures.

The study presented herein novel SC methods such as GPR and ANN together with response surface method (RSM) to estimate the static and dynamic properties of the sedimentary rock based on the experimental datasets obtained from a literature. The P-wave velocity (V_p) and density were used to develop the models for predicting the static and dynamic Young's moduli and UCS of different types of sedimentary rock. The reason for selecting these two parameters is to generate the models that can be easily used for quick assessment of the rock properties as V_p and density are not tedious to be determined in the laboratory. The adopted modelling techniques (such as GPR and RSM) have not been used by any of the previous investigators to simultaneously predict key rock properties from density and V_p to the best of the knowledge of the authors. Hence, reliable models for estimating rock properties are proposed. Detailed sensitivity analysis is also conducted using the RSM method performed in Minitab software. Therefore, the remaining section of the paper is structured in such a way that the overview of the adopted methods is first presented as sub-section under the introduction and thereafter, description of the data source and procedures used in developing the models are presented. This section is followed by the results and discussion section and thereafter the concluding remark.

1.1 Overview of the SC models

1.1.1 Gaussian process regression (GPR)

Gaussian process regression is a nonparametric probabilistic based model that can predict a response variable from a number of variables after undergoing training. This method has been described to be flexible and fully probabilistic by Rasmussen and Williams (2006). As a result, it has been applied in various fields of science and engineering. The probability of the outcome to be predicted is mapped in GPR model by utilizing the mean vector and covariance matrix. Taking the mean of a distribution as μ and σ^2 as the variance, then the probability of the outcome is given as in Eq. (1) for a typical squared exponential function (Bisoyi and Pal 2020). However, Eq. (1) will change for different kernels based on the variation in the covariance function.

$$P(x|\mu,\sigma)=\frac{1}{\sqrt{2\pi\sigma^2}}e^{\frac{-(x-\mu)}{2\sigma^2}} \quad (1)$$

1.1.2 Artificial neural network (ANN)

Artificial neural network is a data driven approach which emulates the function of human brain in manner it receives information, processes it, and relay output of the information. It has been widely used to solve many complex problems in various fields including rock mechanics and mining engineering (Lawal and Idris 2019, Aladejare *et al*. 2020, Lawal 2020, Lawal and Kwon 2020). A typical supervised ANN required an input and targeted variables which are usually from the field measured or experimental datasets. A multilayer feedforward ANN architecture trained with backpropagation training algorithm is the most commonly used in rock mechanics/mining engineering fields. This structure typical consists of one input-one output and one or more hidden layers. Each layer has different number of neurons, the number of neurons in the input layer depends on the model predictors while that of the output depends on the number of dependent variables while the number of neurons in the hidden layers are usually based on trial-and-error approach as there is no established rule agreed upon by the researchers in the literature. The neurons are connected by the weights and biases that are usually associated with the weights. ANN is usually referred to as the black-box approach as the relationship between the input and output is usually less understood. However, in this study, one of the ways to unlock the black-box nature of the ANN is proposed.

2. Materials and method

2.1 Description of the data source

The proposed models were developed using 64 experimental datasets of the core rock samples that are free from the bedding planes from the dam sites in Iran as presented by Moradian and Behnia (2009). The samples were prepared in accordance with the ISRM (1981) standard which is one of the reasons for selecting these datasets for this study. The P-wave and S-wave velocities were determined using the Pundit apparatus while the rock density, uniaxial compressive strength (UCS), static Elastic Modulus and dynamic Elastic modulus were computed based on the relevant recommended rock testing standards. The datasets were determined from seven different dams with varying rock types. All the sites are of sedimentary rocks in nature. Therefore, 44 samples of the entire datasets were obtained from limestone while 12 and 8 samples were respectively from marlstone and sandstone. It can be seen that the data adopted are for sedimentary rocks and are not limited to a specific type of sedimentary rock. Many researchers (for example Moradian and Behnia 2009, Khandelwal and Singh 2009, Sharma *et al*. 2017, Uyanik *et al*. 2019, etc.), have combined data of different rocks in the same family or different family to develop models. The reason is quite straightforward. Most times, there are different rocks in a deposit, especially sedimentary rocks that occur in layers with different rock making up the lithology. Therefore, in many instances, only limited data of different rock types in a lithology are obtained in the laboratory and will be too limited to establish a meaningful relationship or infer any logical conclusion. Hence, the usual practice of combining the data of different rock types making up a sedimentary lithology, and this practice is widely reported in rock mechanics literature (Aladejare *et al*. 2021). Hence, the statistical description of the datasets is presented in Table 2.

Table 2 Description of the datasets (Moradian and Behnia 2009)

	ρ (g/cm^3)	Vp (m/s)	E_s (GPa)	E_d (GPa)	UCS (MPa)
Min	2.04	1826	0.77	4.98	10.24
Max	2.92	6539	90.49	83.89	143.09
Mean	2.51	4005.06	29.35	36.73	56.19
Std	0.21	1611.82	27.57	27.84	33.04
Number of dataset	64	64	64	64	64

2.2 Model developments

Three different models namely: Gaussian process regression (GPR), artificial neural network (ANN), and response surface method (RSM) were proposed for the prediction of static and dynamic properties of different types of sedimentary rock. The details of each of the proposed models are presented below.

2.2.1 Gaussian process regression

The GPR was used in this study to predict the static and dynamic properties of the selected sedimentary rocks using the P-wave velocity and the rock density. The GPR was implemented in MATLAB. Six (6) different covariance functions (CoV) such as rational quadratic (RQard), isotropic squared exponential (iSE), linear (iLIN), Matern 5/2, 1/2, and 3/2 were tried. The detailed information about the GPR and CoV functions can be found in Bisoyi and Pal (2020) and Lawal *et al*. (2021c). The performance of each of the CoV functions for the E_s, E_d, and UCS was tried as presented in Fig. 1. The Matern 1/2 CoV performed better than the remaining CoVs for the three properties while iLIN performed poorly among the CoVs. Hence, results of the GPR model obtained with the Matern 1/2 CoV is compared with the other proposed model in this study.

2.2.2 Artificial neural network (ANN)

ANN described above is also adopted in this study to predict the E_s, E_d, and UCS of different sedimentary rock type. To develop the proposed models for predicting the E_s, E_d, and UCS of three different types of sedimentary rock, two input parameters such as V_p and density were used. That is multi-input and single output feedforward neural network is proposed in this study. The datasets were divided into training and testing/validation datasets (70% for the

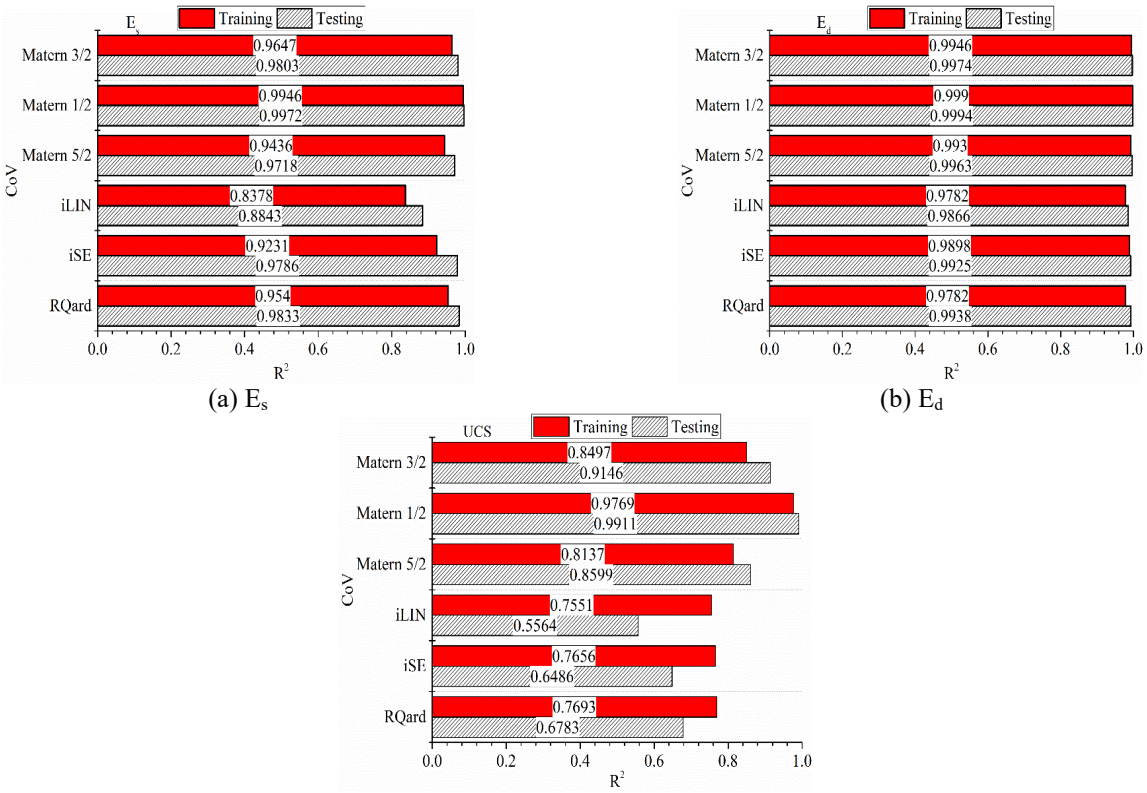

(a) E_s (b) E_d

(c) UCS

Fig. 1 Comparison of different CoV functions

training and 30% for testing/validation). Just before the loading, the datasets were first pre-processed by normalizing them to within the range of -1 and 1, to ensure the uniformity of the datasets and avoid overfitting (Lawal and Idris 2019, Lawal *et al*. 2020). The proposed multi-input and single-output feedforward neural network was then trained using backpropagation algorithm together with Levenberg Marquardt training function. The hyperbolic tangent transfer function was used in both the hidden and output layers. The number of neurons in the input layers for all the three models for E_s, E_d, and UCS predictions were two while the hidden layers were varied between 1 and 10 and the number of output neurons was 1 each for the three models. The ANN networks which performed best for the tried neurons in the hidden layers using the strategy adopted in the case of GPR model (Fig. 1) for each of the properties investigated were selected as the optimum networks. Therefore, the network presented in Fig. 2 was selected as the optimum network for the three rock properties. The outputs of the models are presented in detail under the results section. However, 2-8-1 (Fig. 2(a)) ANN architecture was selected as the optimum network for the E_s while 2-7-1 (Fig. 2(b)) and 2-6-1 (Fig. 2(c)) ANN architectures were selected for the respective E_d and UCS.

2.2.3 Response surface method (RSM)

The RSM is a useful technique for developing, improving, and optimizing processes or products (Myers 2016). It provides absolute values of standardized effects based on Pareto charts with definite reference lines. Moreoever, the magnitude and importance of dependent variables can be revealed using the half normal probability plots. Consequently, the method aims to present dominating factors and interactions on dependent variables (Kowalski and Montgomery 2011). In this regard, the RSM analyses were conducted through Minitab software (Minitab® 18). The linear relationship with interactions (e.g., x_1, x_2, and x_1x_2) was adopted as the fitting function. The ρ and V_p were considered as the dependent variables for E_s, E_d and UCS. Three different RSM models (Model I – III) were established for predicting the E_s, E_d and UCS, respectively. Based on the RSM analysis results, the empirical formula for the estimation of the above-mentioned variables are given by the following equations:

$$E_s = 32.7 - 19.2\rho - 0.0328V_p + 0.0171\rho V_p \text{, GPa} \quad (2)$$

$$E_d = 68.9 - 35.25\rho - 0.02965V_p + 0.01699\rho V_p \text{, GPa} \quad (3)$$

$$UCS = -380 + 157.01\rho - 0.0800V_p + 0.0270\rho V_p \text{, MPa} \quad (4)$$

3. Results and discussion

3.1 Prediction models

The performances of the selected GPR model and the optimum selected ANN model for the E_s, E_d and UCS

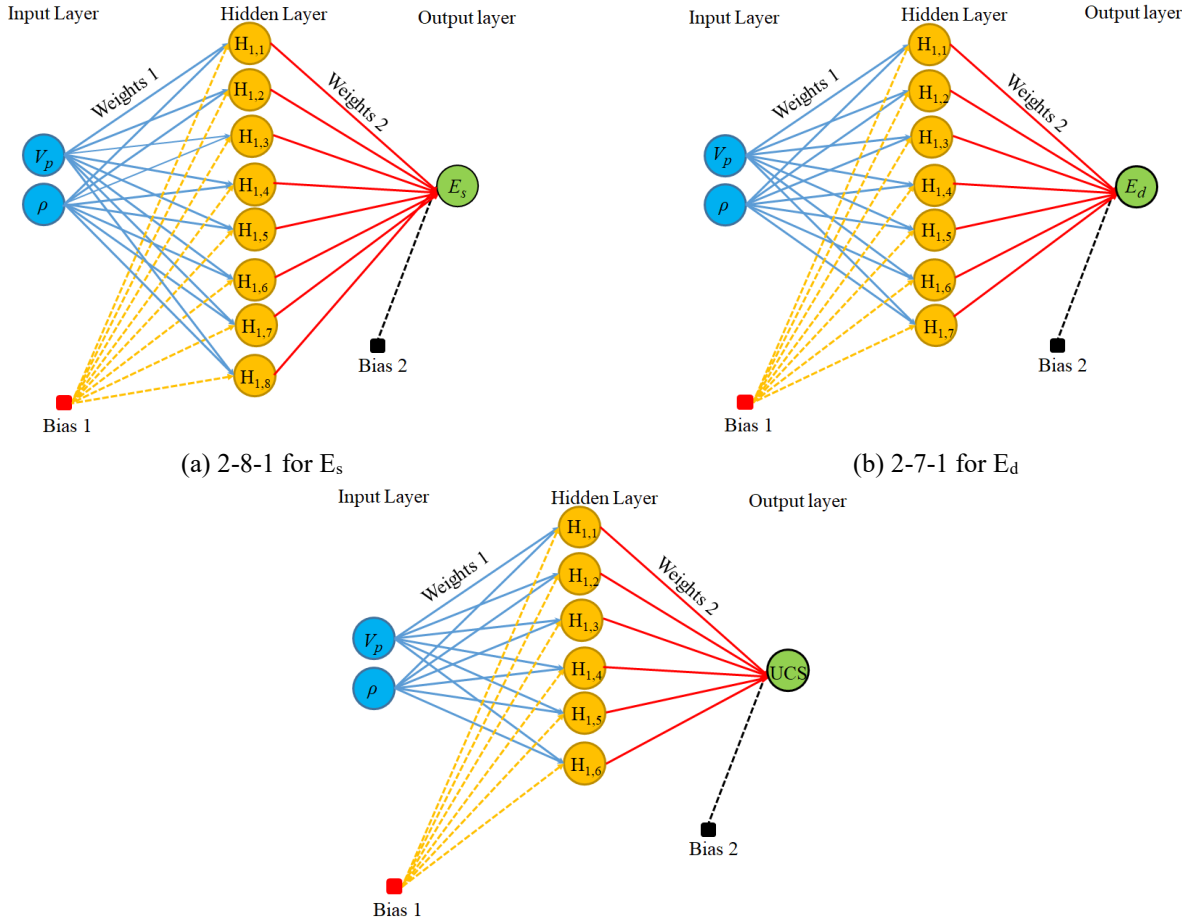

(a) 2-8-1 for E_s

(b) 2-7-1 for E_d

(c) 2-6-1 for UCS

Fig. 2 Optimum ANN structures selected

predictions were evaluated using various statistical indices presented in Eqs. (5) and (6). The RMSE in Eq. (5) measures the error between the actual and predicted variables. The closer the value of RMSE to zero, the better the model performance. Similarly, R-value (Eq. (6)) shows the strength of the relationship between two variables. The R-value of -1 or +1 indicates a perfect relationship while R-value of zero (0) implies that there is no relationship exists between the variables. The closer the values of R to either -1 or 1 the stronger the relationship. However, for the problem under consideration, the negative R-value will imply that the model is poor and cannot be used in predicting the variable of interest since we are correlating the same variables from different sources (that is one experimental and the other from the model).

$$RMSE = \sqrt{\frac{1}{n}\sum_{i=1}^{n}(Exp_i - P_i)^2} \tag{5}$$

$$R = \frac{n\sum Exp_i P_i - \sum Exp_i \sum P_i}{\sqrt{\left(n\sum Exp_i^2 - \left(\sum Exp_i\right)^2\right)\left(n\sum P_i^2 - \left(\sum P_i\right)^2\right)}} \tag{6}$$

where *Exp*, *P*, and *n* are the experimental data, predicted value and the number of data points, respectively. Fig. 3 presents the experimental data points and the GPR predicted data points for the GPR performed using the 1/2 CoV function. The linear least-square fit lines of the training and testing datasets couple with the ideal fit line are also presented in the Fig. 3. The ±5% error bars are also included in Fig. 3. For E_s, E_d, and UCS, the predictions of the proposed models are very close to the experimental values. The predicted data points are largely within the error bars. The statistical performance of the proposed models for the E_s, E_d and UCS is also evaluated as presented in Table 3. The errors obtained are very low while the R-values are very high. These show that the estimates of the static and dynamic mechanical properties of sedimentary rock from the proposed soft computing models are consistent with the measured data of the properties. Note that the reliability of estimates from empirical models increases with increasing R-values and decreasing error value, and vice versa.

3.2 Model comparison

The proposed models in this study are compared with each other in order to determine which of the three proposed models is more suitable for the prediction of the rock mechanical properties prediction. Figs. 4 to 6 depict

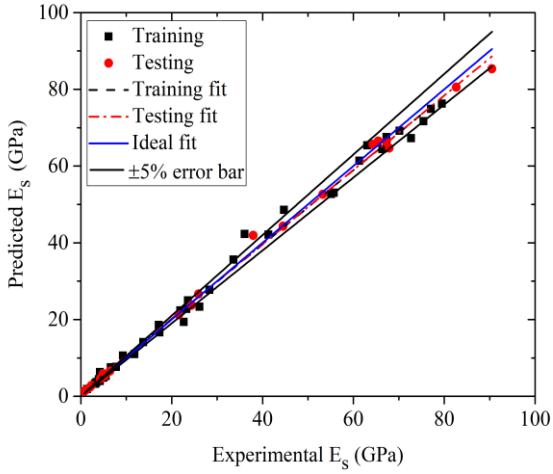

(a) E_s

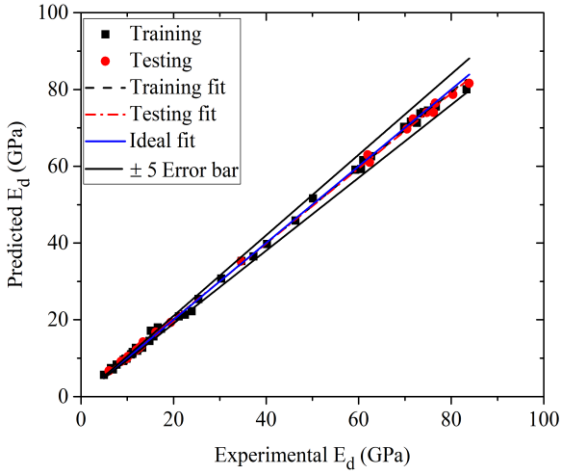

(b) E_d

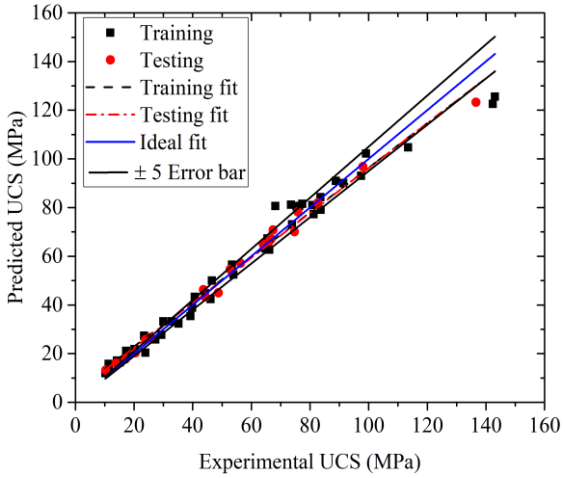

(c) UCS

Fig. 3 Comparing the experimental results with the model predicted training and testing results

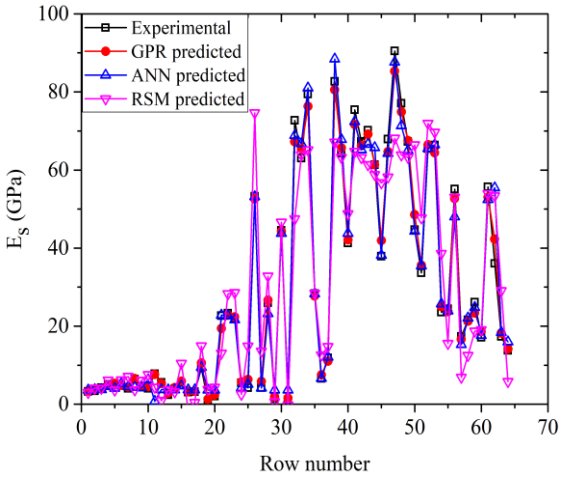

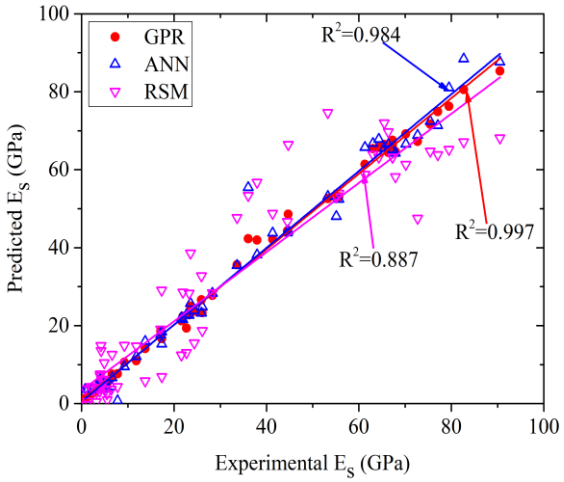

Fig. 4 Comparison of the experimental E_s with the predicted E_s

the plots of the models against the experimental results for the E_s, E_d, and UCS, respectively. Figs 4-6 reveal that GPR model performs better than the other models. Its performance could be attributed to its probabilistic nature. The statistical performances of the models are also evaluated and presented in Table 4. The GPR model has the lowest RMSE and R values follow by ANN and the RSM. The proposed models' performances were also compared with that of Moradian and Behnia (2009) using the UCS case as presented in Table 1. The reason for selecting

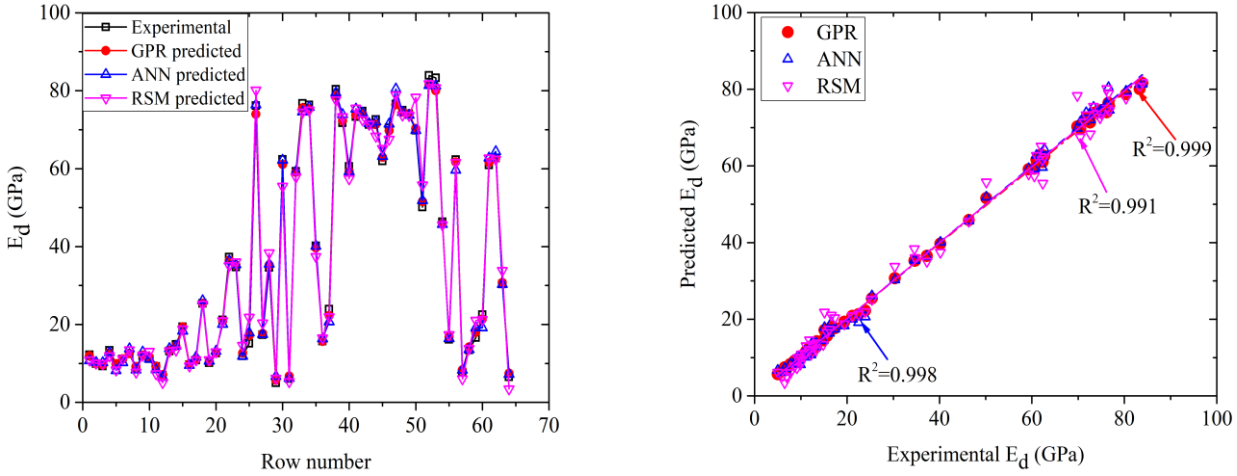

Fig. 5 Comparison of the experimental E_d with the predicted E_d

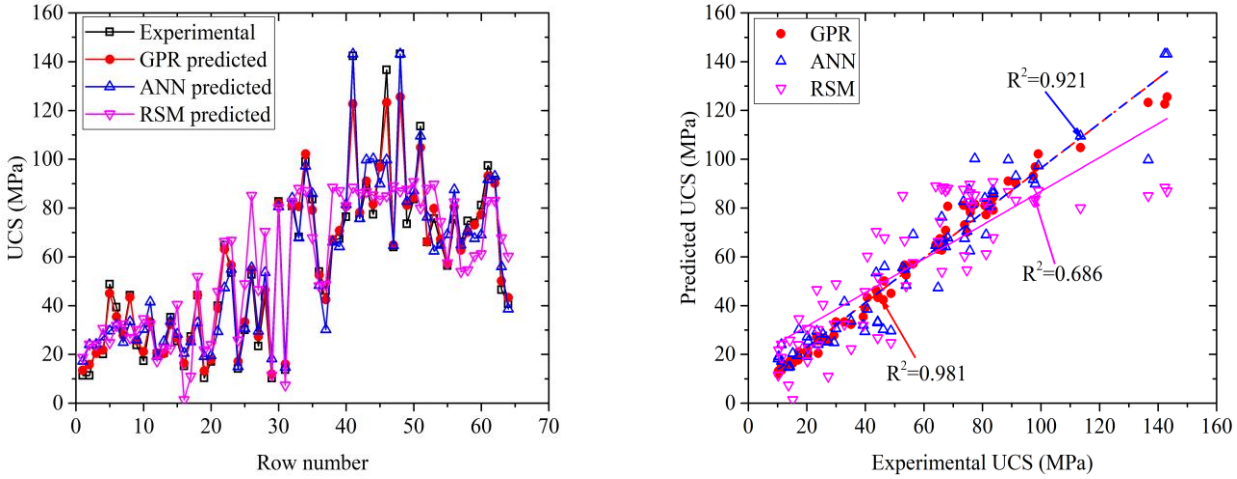

Fig. 6 Comparison of the experimental UCS with the predicted UCS

Table 3 The statistical results of the proposed model

	E_s		E_d		UCS	
	Training	Testing	Training	Testing	Training	Testing
RMSE	2.004	1.800	0.8907	0.9737	5.481	3.627
R	0.997	0.999	0.9995	0.9997	0.988	0.996

Moradian and Behnia (2009) is that the same datasets we adopted in developing our model were also used by Moradian and Behnia (2009). The performance of the GPR and ANN models are better than their proposed model for all the properties investigated.

3.2.1 Taylor's diagram

The Taylor's diagram was published formally by Taylor (2001) for the comparative assessment of several models in a single diagram. The Taylor's diagram is primarily used to establish the degree of correspondence of the observed and modelled behaviours based on three statistics namely: the correlation coefficient, the root-mean squared error and the standard deviation. It was originally used for the climate models and earth's environment related problems but in recent time, various field have been used the Taylor's diagram (Lawal *et al*. 2021d). Similarly in this study, proposed models are compared using the Taylor's diagram combining various statistical indices such as standard deviation, root mean squared error difference and coefficient of correlation. The obtained Taylor's diagram in Fig. 7 was drawn using the MATLAB software. From Fig. 7, GPR appears to be the model with the lowest standard deviation and RMSE with the highest coefficient of correlation follow by ANN models for the three properties investigated while RSM seems to have the lowest performances in predicting the three properties. The three models seem to be good for predicting E_d.

3.3 Sensitivity analysis

The most dominant effects of independent variables in each of the three models developed for predicting E_s, E_d and UCS are studied using the response surface model conducted using Minitab software (Minitab® 18). The detail about the RSM Pareto chart implementation can be found in Köken and Lawal (2021). The outcome of the sensitivity analysis conducted is as presented in Fig. 8. From the

Table 4 Statistically evaluated model performances

Method	E_s			E_d			UCS		
	GPR	ANN	RSM	GPR	ANN	RSM	GPR	ANN	RSM
RMSE	1.942	3.411	9.175	0.917	1.369	2.594	4.976	9.187	18.377
R	0.998	0.992	0.942	0.9996	0.9987	0.9956	0.990	0.960	0.828

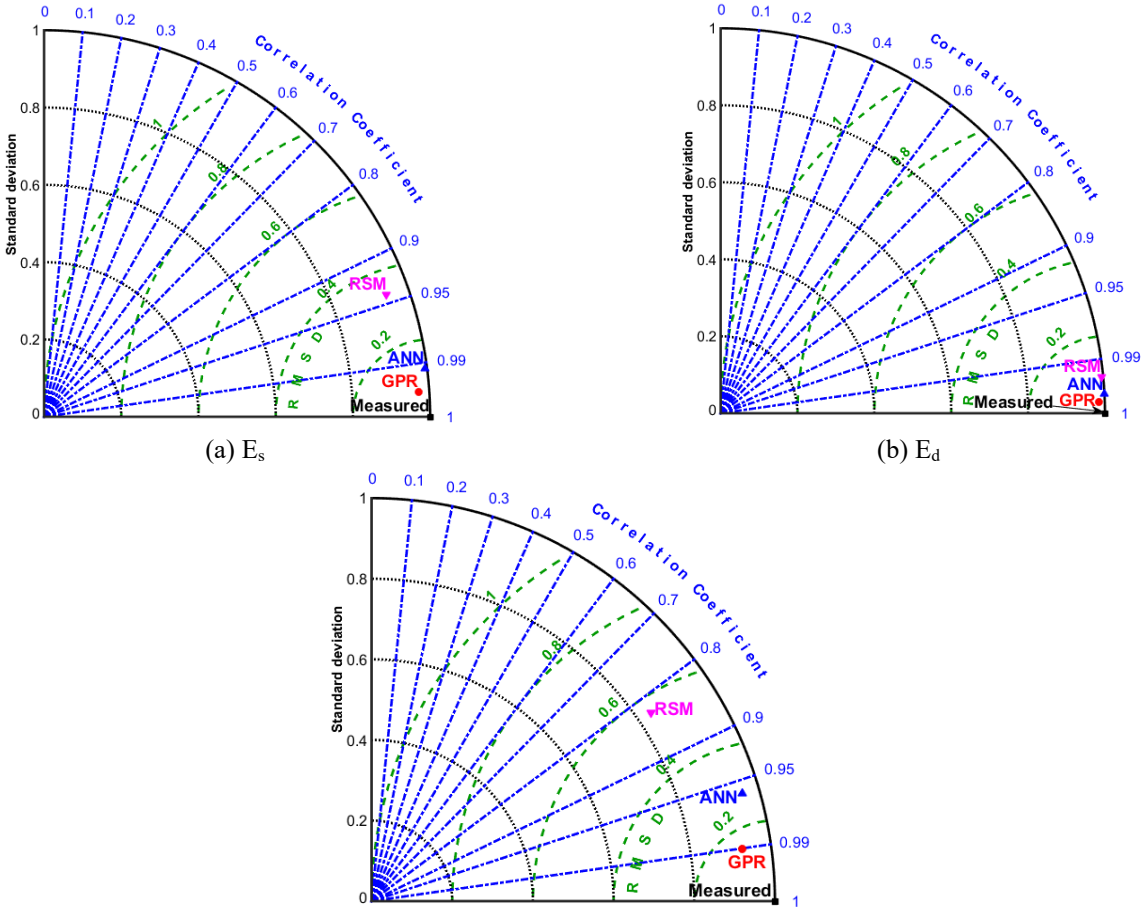

(a) E_s (b) E_d

(c) UCS

Fig. 7 Taylor's diagram showing the performance of the models

figure, it is obvious that the V_p is the most dominating factor for all dependent variables in the context of RSM analyses. The ρ turned out to be a reasonable parameters for the evaluation of the dependent variables. However, for the UCS, neither the ρ nor its interactions were found to be significant parameters (Fig. 8). Because the information contained in each input rock parameter are propagated through model to estimates of E_s, E_d and UCS, the models benefit when the information contained in the dominant parameter is devoid of error as much as possible. For instant, the sensistivity analysis indicates that the estimates of E_s, E_d and UCS from the proposed models will become more confident and reliable as the quality of V_p becomes higher.

3.4 Unlocking the black-box nature of the ANN

One of the demerits of the ANN model is that the interaction between the model inputs and output are not usually understood. This can be solved by transforming the proposed ANN models into mathematical form that can be used for easy prediction of the investigated rock properties without the need to reconstruct a new ANN simulation. This was achieved in this study by extracting the weights and biases of each of the models for the three properties (Table 5).

For the Es, 2-8-1 ANN structure is the optimum and hence the resulting mathematical model is given in Eq. (7).

$$E_s = 44.86 \tanh\left(\sum_{i=1}^{8} x_i \text{-} 5.016\right) + 45.63, \text{GPa} \qquad (7)$$

where x_1 to x_8 are presented as follows;

$$x_1 = 2.3776 \tanh\left(12.6775\rho^n + 14.6523 V_p{}^n - 19.7983\right)$$

$$x_2 = 0.79298 \tanh\left(-2.3636\rho^n + 4.6149 V_p{}^n - 1.6063\right)$$

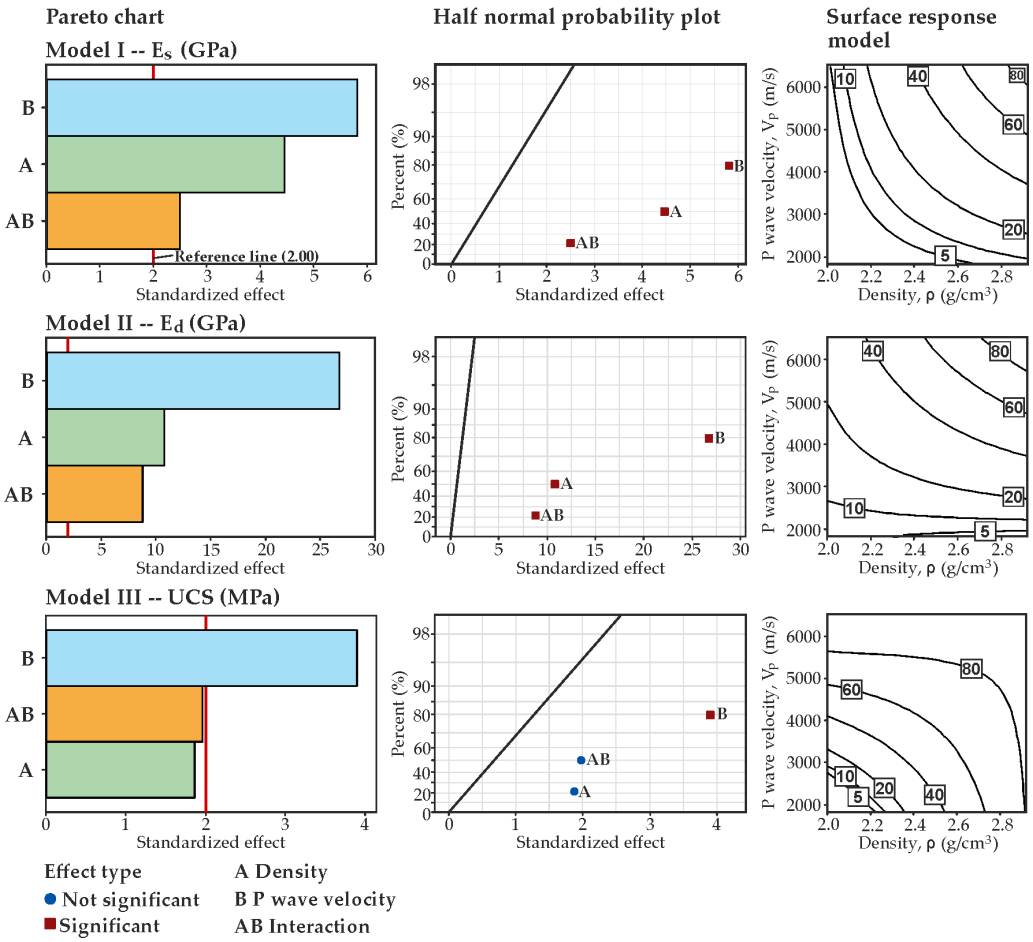

Fig. 8 RSM analysis results

Table 5 Weights and biases of the optimum ANN structures

*HN	Weights 1		Weights 2	Bias 1	Bias 2
			E_s		
1	12.67745	14.65226	2.377604	-19.7983	-5.01615
2	-2.36356	4.614873	0.792983	-1.60629	
3	-32.0982	7.633407	1.935746	14.37443	
4	9.650383	2.025389	21.11953	1.57869	
5	8.916165	17.35238	-1.80365	2.478363	
6	-16.1151	-0.57016	11.81453	-1.32016	
7	-16.844	-2.07941	6.911657	-3.40208	
8	-1.86973	-7.50766	5.13253	8.435164	
			E_d		
1	0.170954	1.084727	6.779454	-1.45795	1.486148
2	6.921168	2.091358	-0.63853	-3.63109	
3	-19.6525	8.433517	5.112477	0.742063	
4	18.55466	-8.08418	5.161923	-0.79397	
5	0.110657	2.05272	2.371536	2.634392	
6	-3.86194	15.39692	-0.34702	-9.41596	
7	-7.60763	7.207065	-1.05556	-4.59151	
			UCS		
1	0.335328	-9.25128	-3.50693	-10.3609	-8.6494
2	92.5986	57.42543	-38.1235	-97.0883	
3	-4.48637	5.417809	1.026634	-0.0536	
4	0.616918	-0.28725	6.286069	0.879365	
5	31.36212	-41.3507	0.431697	4.450464	
6	124.6993	78.59336	37.85938	-131.398	

*HN is the number of hidden neurons

$$x_3 = 1.9357\tanh\left(-32.0982\rho^n + 7.6334V_p{}^n + 1.9357\right)$$
$$x_4 = 21.1195\tanh\left(9.6504\rho^n + 2.0254V_p{}^n + 1.5787\right)$$
$$x_5 = -1.8036\tanh\left(8.9162\rho^n + 17.3524V_p{}^n - 1.3201\right)$$
$$x_6 = 11.8145\tanh\left(-16.1151\rho^n - 0.5702V_p{}^n - 1.3202\right)$$
$$x_7 = 6.9117\tanh\left(-16.8440\rho^n - 2.0794V_p{}^n - 3.4021\right)$$
$$x_8 = 8.4352\tanh\left(-1.8697\rho^n - 7.5077V_p{}^n + 5.1325\right)$$

For the E_d prediction, the 2-7-1 ANN structure is the optimum network and the corresponding mathematical transformation is presented in Eq. (8).

$$E_d = 39.455\tanh\left(\sum_{i=1}^{7} y_i + 1.4861\right) + 44.435\ \text{, GPa} \quad (8)$$

where y_1 to y_7 are given as follows

$$y_1 = 6.7795\tanh\left(0.17095\rho^n + 1.0847V_p{}^n - 1.45795\right)$$
$$y_2 = -0.6385\tanh\left(6.9212\rho^n + 2.0914V_p{}^n - 3.6311\right)$$
$$y_3 = 0.7421\tanh\left(-19.6525\rho^n + 8.4335V_p{}^n + 5.1125\right)$$
$$y_4 = 5.1619\tanh\left(18.5547\rho^n - 8.0842V_p{}^n - 0.79397\right)$$
$$y_5 = 2.3715\tanh\left(0.1107\rho^n + 2.0527V_p{}^n + 2.6344\right)$$

$$y_6 = \text{-}0.347 \tanh\left(-3.8619\rho^n + 15.3969V_p{}^n \text{-} 9.41595\right)$$

$$y_7 = \text{-}1.0556 \tanh\left(-7.6076\rho^n + 7.2071V_p{}^n \text{-} 4.5915\right)$$

Similarly, for the UCS, 2-6-1 ANN structure was selected as the optimum network and the mathematical transformation of the network is presented in Eq. (9).

$$UCS = 66.425 \tanh\left(\sum_{i=1}^{6} z_i - 8.6494\right) + 76.665, \text{ MPa} \quad (9)$$

where z_1 to z_6 are given as below;

$$z_1 = \text{-}3.5069 \tanh\left(0.3353\rho^n - 9.2513V_p{}^n \text{-} 10.3609\right)$$

$$z_2 = \text{-}38.1235 \tanh\left(92.5986\rho^n + 57.4254V_p{}^n \text{-} 97.0882\right)$$

$$z_3 = 1.0266 \tanh\left(-4.4864\rho^n + 5.4178V_p{}^n \text{-} 0.0536\right)$$

$$z_4 = 6.2861 \tanh\left(0.6169\rho^n - 0.2872V_p{}^n + 0.8794\right)$$

$$z_5 = 0.4317 \tanh\left(31.3621\rho^n - 41.3507V_p{}^n + 5.4504\right)$$

$$z_6 = 37.8594 \tanh\left(124.6993\rho^n + 78.5934V_p{}^n \text{-} 131.3975\right)$$

The ρ^n and $V_p{}^n$ in the equations are their normalized values which are given as $\rho^n = 2(\rho\text{-}2.04)/0.88\text{-}1$ and $V_p{}^n = 2(V_p\text{-}1826)/4713\text{-}1$ respectively. The Eqs. (7)-(9) present above are direct replicate of the ANN predictions for E_s, E_d, and UCS respectively.

4. Conclusions

The study proposed soft computing models for the prediction of the static and dynamic properties of different types of sedimentary rock. The models are developed to tackle the bottlenecks (i.e., sample preparation tasks, time and cost of experimentation, etc.) associated with the direct determination of static and dynamic Youngs' modulus and uniaxial compressive strength.

The proposed models are the GPR, ANN, and RSM models, which were developed using the 64 datasets obtained from literature. The datasets were first normalized and then divided into the training and validation datasets using the recommended ratio in the case of GPR and ANN model developments. The performances of the models were evaluated using statistical indices such as correlation coefficient and root mean squared error. Sensitivity analysis was also performed using the RSM technique. In addition, the black-box nature of the ANN was also unlocked by mathematically transforming the ANN predictions into simple mathematical forms

The R-values of the three models are very high for the three properties estimated. The R-values are greater than 0.9 in all cases, except for the estimation of UCS using RSM model where R-value is less than 0.9. In addition, the RMSE values for the estimations of the three properties are relatively low with values lower than 10, except in UCS estimation using RSM model where it is substantially greater than 10.

Hence, from the outcomes of the study, the following conclusions can be drawn as follows:

- All the models performed well in dynamic Young's modulus predictions. However, the predictions of UCS contain noticeable error, which is exceptionally high in the case of RSM model.
- The GPR model performed better than the other models in all the parameters predicted, with the least RMSE and the highest R-values in all the properties estimated.
- Sensitivity analysis showed that V_p is the most influencing parameters in E_s, E_d, and UCS prediction models.
- RSM can also serve as a useful method for predicting the rock properties, especially because of its easy and efficient practical implementation.
- The merit of using GPR, ANN, and RSM models in rock engineering is their robustness and ability to incorporate the variabilities in rock properties in their property estimation, which is not achievable with simple or multiple regression models.

Acknowledgments

This work was supported by Korea Research Fellowship Program through the National Research Foundation of Korea (NRF) funded by the Ministry of Science and ICT (2019H1D3A1A01102993) and Inha University Research Grant (2021).

References

Aboutaleb, S., Behnia, M., Bagherpour, R. and Bluekian, B. (2018), "Using non-destructive tests for estimating uniaxial compressive strength and static Young's modulus of carbonate rocks via some modeling techniques", *Bull. Eng. Geol. Environ.*, **77**(4), 1717-1728. https://doi.org/10.1007/s10064-017-1043-2.

Aladejare, A.E. (2020), "Evaluation of empirical estimation of uniaxial compressive strength of rock using measurements from index and physical tests", *J. Rock Mech. Geotech. Eng.*, **12**(2), 256-268. https://doi.org/10.1016/j.jrmge.2019.08.001.

Aladejare, A.E., Kärenlamp, K. and Lawal, A.I. (2020), "Application of Artificial Intelligence for Characterization of Rocks from Otanmäki, Finland", *Proceedings of the 54th US Rock Mechanics/Geomechanics Symposium. American Rock Mechanics Association*.

Aladejare, A.E., Alofe, E.D., Onifade, M., Lawal, A.I., Ozoji, T.M. and Zhang, Z.-X. (2021), "Empirical estimation of uniaxial compressive strength of rock: database of simple, multiple, and artificial intelligence-based regressions", *Geotech. Geol. Eng.*, **39**, 4427-4455. https://doi.org/10.1007/s10706-021-01772-5.

Aliyu, M.M., Shang, J., Murphy, W., Lawrence, J.A., Collier, R., Kong, F. and Zhao, Z. (2019), "Assessing the uniaxial compressive strength of extremely hard cryptocrystalline flint", *Int. J. Rock Mech. Min. Sci.*, **113**, 310-321. https://doi.org/10.1016/j.ijrmms.2018.12.002.

Armaghani, D.J., Mohamad, E.T., Momeni, E., Narayanasamy, M. S. (2015), "An adaptive neuro-fuzzy inference system for predicting unconfined compressive strength and Young's modulus: A study on Main Range granite", *Bull Eng Geol Environ*, **74**(4):1301-1319. https://doi.org/10.1007/s10064-014-0687-4.

Armaghani, D.J., Mohamad, E.T., Hajihassani, M., Yagiz, S. and

Motaghedi, H. (2016), "Application of several non-linear prediction tools for estimating uniaxial compressive strength of granitic rocks and comparison of their performances", *Eng. Comput*., **32**(2), 189-206. https://doi.org/10.1007/s00366-015-0410-5.

Armaghani, D.J., Safari, V., Fahimifar, A., Monjezi, M. and Mohammadi, M.A. (2018), "Uniaxial compressive strength prediction through a new technique based on gene expression programming", *Neural Comput. Appl*., **30**(11), 3523-3352. https://doi.org/10.1007/s00521-017-2939-2.

Armaghani, D.J., Mamou, A., Maraveas, C., Roussis, P.C., Siorikis, V.G., Skentou, A.D. and Asteris, P.G. (2021), "Predicting the unconfined compressive strength of granite using only two non-destructive test indexes", *Geomech. Eng*., **25**(4), 317-330. https://doi.org/10.12989/gae.2021.25.4.317.

Azimian, A., Ajalloeian, R. and Fatehi, L. (2014), "An empirical correlation of uniaxial compressive strngth with P-wave velocity and point load strength index on marly rocks using statistical method", *J. Geotech. Geol. Eng*., **32**, 205-214. https://doi.org/10.1007/s10706-013-9703-x.

Ashtari, M., Mousavi, S.E., Cheshomi, A. and Khamechian, M. (2019), "Evaluation of the single compressive strength test in estimating uniaxial compressive and Brazilian tensile strengths and elastic modulus of marlstone", *Eng. Geol*., **248**, 256-266. https://doi.org/10.1016/j.enggeo.2018.12.005.

Bisoyi, S.K. and Pal, B.K. (2020), "Prediction of ground vibration using various regression analysis", *J. Min. Sci*., **56**(3), 378-387. https://doi.org/10.1134/S1062739120036665.

Dincer, I., Acar, A. and Ural, S. (2008), "Estimation of strength and deformation properties of Quaternary caliche deposits", *Bull. Eng. Geol. Environ.*, **63**, 141-148. https://doi.org/10.1007/s10064-008-0146-1.

Heidari, M., Mohseni, H. and Jalali, S.H. (2018), "Prediction of Uniaxial Compressive Strength of Some Sedimentary Rocks by Fuzzy and Regression Models", *Geotech. Geol. Eng*., **36**, 401-412. https://doi.org/10.1007/s10706-017-0334-5.

International Society for Rock Mechanics (ISRM) (1981), *Suggested methods. Rock characterization testing and monitoring*, E. T. Brown, ed., Pergamon, Oxford, U.K.

Jalali, S.H., Heidari, M. and Mohseni, H. (2017), "Comparison of models for estimating uniaxial compressive strength of some sedimentary rocks from Qom Formation", *Environ. Earth Sci*., **76**, 753. https://doi.org/10.1007/s12665-017-7090-y.

Jamshidi, A., Zamanian, H., Sahamieh, R.Z. (2018), "The effect of density and porosity on the correlation between uniaxial compressive strength and P-wave velocity", *Rock Mech. Rock Eng*., **51**, 1279-1286. https://doi.org/10.1007/s00603-017-1379-8.

Khandelwal, M. and Singh, T.N. (2009), "Correlating static properties of coal measures rocks with P-wave velocity", *Int. J. Coal Geol*., **79**(1-2), 55-60. https://doi.org/10.1016/j.coal.2009.01.004.

Köken, E. and Lawal, A.I. (2021), "Investigating the effects of feeding properties on rock breakage by jaw crusher using response surface method and gene expression programming", *Adv Powd Tech*., **32**, 1521-1531. https://doi.org/10.1016/j.apt.2021.03.007.

Kowalski S.M. and Montgomery D.C. (2011), *Design and analysis of experiments, Minitab manual*. 7th Ed., Wiley, ISBN: 978-0-470-16990-2.

Lawal, A.I. and Idris, M.A. (2019), "An artificial neural network-based mathematical model for the prediction of blast-induced ground vibrations", *Int. J. Environ Std.*, **77**(2), 318-334. https://doi.org/10.1080/00207233.2019.1662186.

Lawal, A.I. and Kwon, S. (2020), "Application of artificial intelligence in rock mechanics: an overview", *J. Rock Mech. Geotech. Eng*., **13**, 248-266. https://doi.org/10.1016/j.jrmge.2020.05.010.

Lawal, A.I. (2020), "An artificial neural network-based mathematical model for the prediction of blast-induced ground vibration in granite quarries in Ibadan, Oyo State, Nigeria", *Sci. African*, **8**, e00413. https://doi.org/10.1016/j.sciaf.2020.e00413.

Lawal, A.I., Kwon, S. and Kim, G.Y. (2021a), "Prediction of the blast-induced ground vibration in tunnel blasting using ANN, metaheuristic ANNs and gene expression programming". *Acta Geophys*., **69**, 161-174. https://doi.org/10.1007/s11600-020-00532-y.

Lawal, A.I., Kwon, S., Hammed, O.S. and Idris, M.A. (2021b), "Blast-induced ground vibration prediction in granite quarries: An application of Gene expression programming, ANFIS, and Sine Cosine algorithm optimized ANN", *Int. J. Mining Sci. Tech*., **31**, 265-277. https://doi.org/10.1016/j.ijmst.2021.01.007.

Lawal, A.I., Olajuyi, S.I., Kwon, S., Aladejare E.A. and Edo, T.M. (2021c), "Prediction of blast-induced ground vibration using GPR and blast-design parameters optimization based on novel grey-wolf optimization algorithm", *Acta Geophys*., **69**, 1313-1324. https://doi.org/10.1007/s11600-021-00607-4.

Lawal, A.I., Oniyide, G.O., Kwon, S., Onifade, M., Köken, E. and Ogunsola, N.O. (2021d), "Prediction of mechanical properties of coal from non-destructive properties: A comparative application of MARS, ANN, and GA", *Nat. Resour. Res*., **30**, 4547-4563. https://doi.org/10.1007/s11053-021-09955-w.

Luat, N.V., Lee, K. and Thai, D.K. (2020), "Application of artificial neural networks in settlement prediction of shallow foundations on sandy soils", *Geomech. Eng*., **20**(5), 385-397. http://dx.doi.org/10.12989/gae.2020.20.5.385.

Majdi, A. and Rezaei, M. (2013), "Prediction of unconfined compressive strength of rock surrounding a roadway using artificial neural network", *Neural Comput. Appl*., **23**, 381-389. https://doi.org/10.1007/s00521-012-0925-2.

Majdi, A. and Beiki, M. (2010), "Evolving neural network using a genetic algorithm for predicting the deformation modulus of rock masses", *Int. J. Rock Mech. Min. Sci*., **47**(2), 246-253. https://doi.org/10.1016/j.ijrmms.2009.09.011.

Mohamad, E.T., Armaghani, D.J., Momeni, E. and Abad S. (2015), "Prediction of the unconfined compressive strength of soft rocks: A PSO-based ANN approach", *Bull. Eng. Geol. Environ.*, **74**(3), 745–757. https://doi.org/10.1007/s10064-014-0638-0.

Mohamad, E.T., Armaghani, D.J., Momeni, E., Yazdavar, A.H. and Ebrahimi, M. (2018), "Rock strength estimation: a PSO-based BP approach", *Neural Comput. Appl*., **30**(5), 1635-1646. https://doi.org/10.1007/s00521-016-2728-3.

Moradian, Z.A. and Behnia, M. (2009), "Predicting the Uniaxial Compressive Strength and Static Young's Modulus of Intact Sedimentary Rocks Using the Ultrasonic Test", *Int. J. Geomech*., **9**(1), 14-19. https://doi.org/10.1061/(ASCE)1532-3641(2009)9:1(14).

Myers, R.H. (2016), *Response surface methodology: Process and product optimization using designed experiments*, 4th ed. (Raymond H. Myers, Douglas C. Montgomery, Christine M. Anderson-Cook. Eds.), Wiley, ISBN 978-1-118-91601-8.

Rasmussen, C.E. and Williams, C.K.I (2006), *Gaussian processes for machine learning*, The MIT Press, Cambridge.

Ren, Q., Wang, G., Li, M. and Han, S. (2019), "Prediction of rock compressive strength using machine learning algorithms based on spectrum analysis of geological hammer". *Geotech. Geol. Eng*., **37**, 475-489. https://doi.org/10.1007/s10706-018-0624-6.

Sharma, L.K., Vishal, V. and Singh, T.N. (2017), "Developing novel models using neural networks and fuzzy systems for the prediction of strength of rocks from key geomechanical properties", *Meas*., **102**, 158-169. https://doi.org/10.1016/j.measurement.2017.01.043.

Taylor, K.E. (2001), "Summarizing multiple aspects of model performance in a single diagram", *J. Geophys. Res*., **106**, 7183-

7192. https://doi.org/10.1029/2000JD900719.
Torabi, S.R., Ataei, M. and Javanshir, M. (2010), "Application of Schmidt rebound number for estimating rock strength under specific geological conditions", *J. Min. Environ*, **1**(2), 1-8. https://doi.org/10.22044/jme.2011.9.
Uyanik, O., Sabbag, N., Uyanik, N.A. and Oncu, Z. (2019), "Prediction of mechanical and physical properties of some sedimentary rocks from ultrasonic velocities". *Bull. Eng. Geol. Environ.*, **78**, 6003-6016. https://doi.org/10.1007/s10064-019-01501-6.
Yılmaz, I. and Yuksek, A.G. (2018), "An example of artificial neural network (ANN) application for indirect estimation of rock parameters", *Rock Mech. Rock Eng*., **41**(5), 781-795. https://doi.org/10.1007/s00603-007-0138-7.
Zorlu, K., Gokceoglu, C., Ocakoglu, F., Nefeslioglu, H.A. and Acikalin, S. (2008), "Prediction of uniaxial compressive strength of sandstones using petrography-based models", *Eng. Geol*., **96**(3-4), 141-158. https://doi.org/10.1016/j.enggeo.2007.10.009.

IC